Tunable Nanoarchitectures

DOI: 10.1002/anie.201007433

Tunable, Discrete, Three-Dimensional Hybrid Nanoarchitectures**

Feng Li, Ding Gao, Xiaomin Zhai, Yanhua Chen, Tao Fu, Dongmin Wu, Zhi-Ping Zhang, Xian-En Zhang, and Qiangbin Wang**

Discrete nanoparticle (NP) ensembles have attracted increasing attention because of their potential in fundamental research and novel functional devices. For example, discrete gold and silver NP dimers displayed strong plasmon coupling and functioned as molecular rulers.[1] Self-assembly is a powerful and widely used route to construct discrete superstructures of NPs.[2] To tailor the components and conformation of such structures, different strategies have been explored to guide NP self-assembly. Small molecules and peptides have proven their efficacy in forming various nanostructures but are restricted to organizing NPs into one-dimensional (1D) and 2D nanostructures.[3–5] DNA provides a better platform for guiding assembly of 3D as well as 1D and 2D nanostructures.[6–11] Recently, pyramidal[12] and tubular[13] nanoarchitectures were constructed by assembling unitary or binary NPs with DNA as scaffold. However, a robust platform for controlling 3D NP assembly with finer tunability still remains a challenge. An ideal strategy to assemble discrete 3D nanoarchitectures should offer 1) tunability of particle species, particle number, and interparticle distance in a single ensemble, 2) good stability, and 3) high yield of products.

Proteins can be composed of more than twenty different amino acid residues and thus have much greater structural diversity than DNA. Various protein structures such as shells, fibers, tubes, and layers have been found in nature and can perform as potential templates, containers, and scaffolds for building nanostructures.[14–17] Moreover, proteins can be genetically engineered to introduce functional amino acids into specific sites, which enables precise control of the organization of rationally designed nanostructures. Virus-based NPs (VNPs) are spherical shells formed by viral capsid proteins. Due to the uniform nanoscale size, symmetric structure, controllable self-assembly, easy fabrication, and modification, VNPs are recognized as effective nanoworkbenches.[18–25] Here we report controllable assembly of discrete 3D nanoarchitectures of quantum dots (QDs) and gold nanoparticles (AuNPs) with mutated VNPs as scaffolds by simultaneous use of their inside and outside space. The VNPs were formed by the major capsid protein of simian virus 40 (SV40), VP1. The assembly process consists of two steps: I) loading QDs into VNPs and II) attaching AuNPs to VNP surfaces (Figure 1).

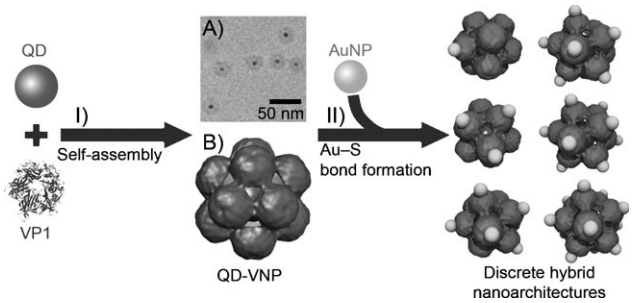

Figure 1. VNP-templated assembly of 3D discrete hybrid Au/QD nanoarchitectures. A) Cryo-TEM image of QD-VNPs. B) 3D reconstructed image of QD-VNPs.

First, QDs coated with 3-mercaptopropionic acid (MPA) were encapsulated in VNPs in a highly efficient manner by molecular self-assembly, with one QD center per VNP (Figure 1 A). The as-prepared QD-containing VNPs (QD-VNPs) are about 24 nm in diameter and consist of twelve VP1 pentamers with $T=1$ icosahedral symmetry (T is the triangulation number, indicating the rules for arranging the subunits on a surface lattice[26]), which was revealed by cryo transmission electron microscopy (cryo-TEM) and 3D reconstruction (Figure 1 B).

Second, different numbers of citrate-capped AuNPs (4.2 nm in diameter) were controllably assembled onto the outer surface of QD-VNPs to obtain discrete 3D nanoarchitectures. To achieve high affinity of AuNPs to the VNPs, alanine 74 of VP1 was substituted by cysteine in step I so that

[*] Dr. F. Li, Dr. X. Zhai, Y. Chen, Dr. T. Fu, Prof. Dr. D. Wu, Prof. Dr. Q. Wang
Division of Nanobiomedicine and*i*-Lab
Suzhou Institute of Nano-Tech and Nano-Bionics
Chinese Academy of Sciences, Suzhou, 215123 (China)
Fax: (+86) 512-6287-2620
E-mail: qbwang2008@sinano.ac.cn
D. Gao, Prof. Z. P. Zhang, Prof. Dr. X. E. Zhang
State Key Laboratory of Virology, Wuhan Institute of Virology, Chinese Academy of Sciences
Wuhan, 430071 (China)
Fax: (+86) 27-8719-9492
E-mail: x.zhang@wh.iov.cn

[**] F.L. acknowledges funding by NSFC (Grant No. 31040032); Q.W acknowledges funding by the "Bairen Ji Hua" program from CAS, MOST (Grant No. 2011CB965004), NSFC (Grant No. 20173225, 91023038), and CAS/SAFEA International Partnership Program for Creative Research Teams; Z.Z. thanks funding by MOST (Grant No. 2011CB933600). The authors thank Peidong Yang at UC Berkeley for helpful discussions; Gang Ji and Lijun Bi at Institute of Biophysics, CAS for assistance in cryo-TEM sampling and testing; Haomiao Zhu and Xueyuan Chen at Fujian Institute of Research on the Structure of Matter, CAS for help with time-resolved fluorescence measurement; and Wen Zhao for 3D drawings. The authors express their appreciation to Electron Microscope Lab at Suzhou Institute of Nano-Tech and Nano-Bionics, CAS for the TEM facilities used in this research.

Supporting information for this article is available on the WWW under http://dx.doi.org/10.1002/anie.201007433.

the VNPs display semi-exposed thiol groups in accordance with the structure of VP1 pentamer[27] (see Supporting Information). In the mutated QD-VNPs, each pentamer provides five thiol groups for capturing one AuNP with high affinity. Compared with the reported methods, VNPs have the intrinsic advantages of rigid 3D conformation and robustness against pH, as well as buffer ion strength. A critical issue in step II is how to prevent the Au/QD-VNP nanoarchitectures from agglomeration due to cross-linking among QD-VNPs and AuNPs. The state of dispersion of the Au/QD-VNP nanoarchitectures depends on the competition between the binding affinity of cysteine residues on QD-VNPs to AuNPs and the electrostatic repulsion and steric hindrance of QD-VNPs. In this work, the binding affinity and steric hindrance are fixed parameters, since the physicochemical properties of QD-VNPs and AuNPs were constant. Therefore, the state of dispersion can be regulated by changing the pH, which determines the electrostatic repulsion among QD-VNPs. A pH value around 6 was optimum to achieve good dispersion of the hybrid Au/QD-VNP nanoarchitectures. The zeta potential of QD-VNPs at pH 6 was measured to be (-22.4 ± 3.7) mV, which stabilized the QD-VNPs during the assembly process and was suitable for AuNP binding to QD-VNPs through gold–sulfur bond formation.

Figure 2 shows that the tunable hybrid Au/QD nanoarchitectures can be obtained in high yields by precisely controlling the ratio of AuNPs to QD-VNPs. Particle numbers of AuNPs per cluster (PNAC) of 1, 3, 5, 6, 8, 10, and 12 were achieved (see Supporting Information for more TEM images). The QDs are not visible in Figure 2 because their electron contrast is lower than that of AuNPs. The histograms in Figure 2, obtained by statistically analyzing about 100 samples, show narrow PNAC distributions. Moreover, the PNACs of all clusters were found to be linearly correlated to the preset molar ratio of AuNPs to QD-VNPs (Figure 2H). These observations demonstrate that the VNP can be utilized as a robust scaffold to precisely assemble discrete 3D hybrid Au/QD nanoarchitectures. In comparison

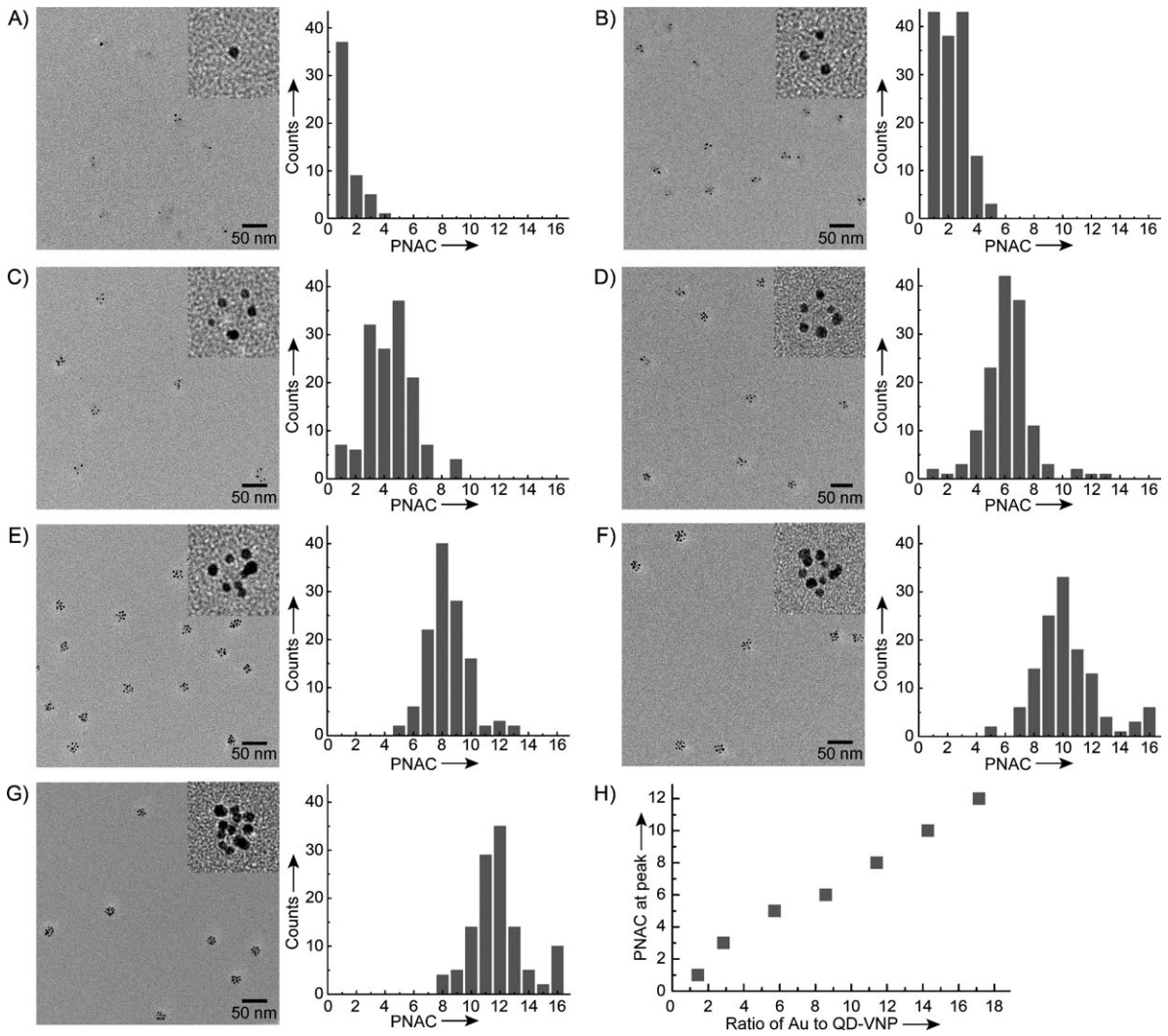

Figure 2. Typical TEM images of Au/QD-VNP nanoarchitectures and histograms of the distribution of PNAC. Inset: high-magnification TEM image of a single Au/QD-VNP entity. A)–G) As-prepared nanoarchitectures with PNACs of 1, 3, 5, 6, 8, 10, and 12, respectively. H) Correlation between PNAC and AuNP/QD-VNP ratio.

with DNA scaffolds, which usually give low yields due to use of electrophoresis for product purification, the simplicity of VNP-based self-assembly endows this strategy with high yield and high reproducibility, and facilitates construction of discrete hybrid nanoarchitectures and further investigation of interactions between different NPs thereof.

The interaction of the AuNPs with each other is of interest, since AuNPs are located on the VNP within close proximity, which may allow surface plasmon resonance (SPR) coupling to occur and cause a redshift of the surface plasmon band.[2] The SPR coupling effect mainly depends on interparticle distance and particle diameter[28] and has been experimentally studied for 2D noble metal NP arrays.[1,29] Absorption spectra of Au/QD-VNP nanoarchitectures with PNAC = 1, 3, 5, 6, 8, 10, and 12 are compared with those of free AuNPs as references in Figure 3A. As summarized in Figure 3B, the absorption redshift gradually increased to 5 nm as the PNAC increased from 1 to 12. This suggests that weak SPR coupling takes place among the 4.2 nm-sized AuNPs. The discrete dipole approximation was adopted to theoretically simulate the plasmon coupling effect of the AuNPs assembled on VNP surfaces. The results also confirmed that plasmon coupling occurred, albeit to a small extent, because the role of phase retardation and multiple-mode effects can be neglected for quasistatic particles.[30]

Quantitative study of the interaction between surface plasmons of metal NPs and fluorescent nanocrystals is of great importance and has drawn intense attention in the past decades.[31–35] The as-obtained hybrid Au/QD-VNP nanoarchitectures provide a robust platform for such studies, since a single QD is surrounded by tunable numbers of AuNPs at a fixed distance (ca. 8 nm). Steady-state fluorescence was first measured for all of the obtained discrete samples (see Supporting Information). Because the fluorescence of QDs can be affected by absorption of the incident light by the AuNPs and the QD-emitted light in the hybrid Au/QD-VNP nanoarchitectures, mixtures of free QDs and AuNPs were used as references to evaluate such effects.

As shown in Figure 4A, the fluorescence intensity of QDs in the references decreased slowly with increasing Au/QD ratio. In contrast, for the hybrid Au/QD-VNP nanoarchitectures, the fluorescence intensity of the VNP-capped QDs dropped dramatically with increasing PNAC, which can be attributed to increased energy transfer from QD to the surrounding AuNPs. Theoretical calculations of the quenching effect of AuNPs on QDs (see Supporting Information for details) showed high similarity to the experimental data. Consistently, time-resolved fluorescence measurements showed that the lifetimes of QDs in the hybrid nanoarchi-

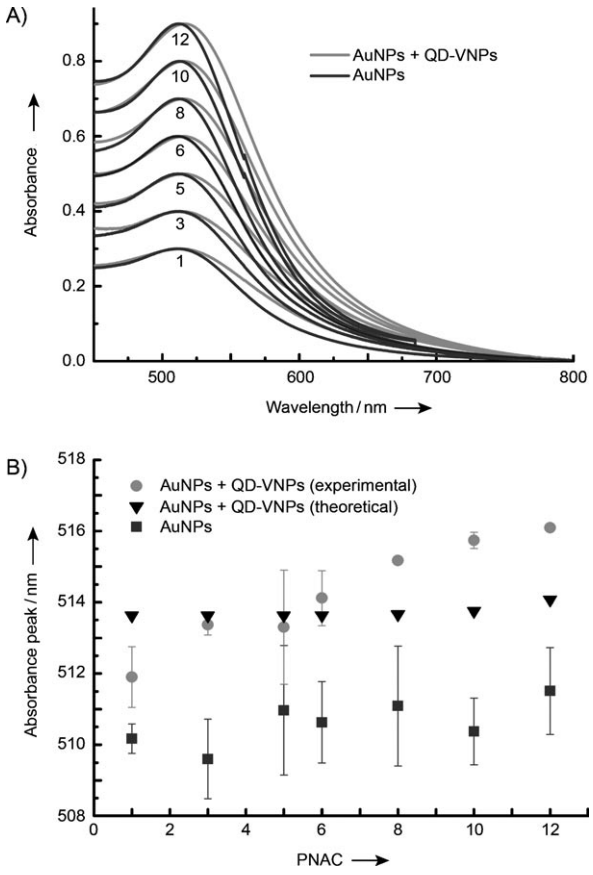

Figure 3. Effect of PNAC on the absorbance of Au/QD-VNP nanoarchitectures, from which the contribution of QDs has been subtracted. A) Absorbance spectra of AuNP clusters compared with those of free AuNPs. The curve parameter is PNAC. The controls are free AuNPs at the same concentration as those in the corresponding clusters. B) Summary of absorbance peaks for AuNP clusters and free AuNPs.

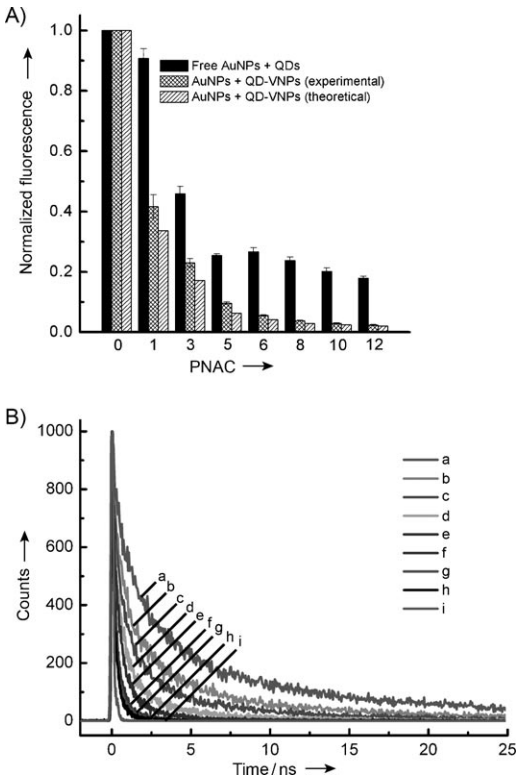

Figure 4. Effect of AuNPs on the fluorescence of VNP-capped QDs. A) Fluorescence intensity of QDs with different numbers of AuNPs. B) Time-resolved fluorescence measurements on a) QD-VNPs; b)–h) QD-VNPs with PNACs of 1, 3, 5, 6, 8, 10 and 12; i) instrument response.

tectures gradually became shorter as the number of AuNPs on the VNP increased (Figure 4B), while those of the references (free QDs and AuNPs) remained nearly unchanged (see Supporting Information).

In summary, we have obtained a series of discrete 3D hybrid Au/QD nanoarchitectures with VNPs as scaffold, which have a central QD and a tunable number of surrounding AuNPs (1, 3, 5, 6, 8, 10, and 12). Thus, VNPs can serve as robust scaffolds for controllably guiding the self-assembly of 3D nanoarchitectures. The well-defined symmetry and size, together with addressable functionalities of VNPs through rational design and genetic engineering, offer precise control of particle species and number, interparticle distance, and conformation. This VNP-based strategy is versatile because 1) a variety of viruses can be exploited to assemble NPs[36] and 2) a wealth of NPs with different components and different sizes[37–38] can be assembled. We expect that this strategy will provide perfect control over the number and tropism of NPs in a single entity when highly selective functionalization of the VNP surface is achieved. VNP-guided NP assembly can be extended to other methods based on protein structure and may find application in biosensing, controllable delivery of bioactive molecules, energy harvesting, and so on.

Received: November 26, 2010
Published online: April 6, 2011

Keywords: gold nanoparticles · quantum dots · self-assembly · viruses

[1] C. Sönnichsen, B. M. Reinhard, J. Liphardt, A. P. Alivisatos, *Nat. Biotechnol.* **2005**, *23*, 741 – 745.
[2] Z. Nie, A. Petukhova, E. Kumacheva, *Nat. Nanotechnol.* **2010**, *5*, 15 – 25.
[3] W. Maneeprakorn, M. A. Malik, P. O'Brien, *J. Am. Chem. Soc.* **2010**, *132*, 1780 – 1781.
[4] C. L. Chen, N. L. Rosi, *J. Am. Chem. Soc.* **2010**, *132*, 6902 – 6903.
[5] M. E. H. Li, M. O'Keeffe, O. M. Yaghi, *Nature* **1999**, *402*, 276 – 279.
[6] H. Gu, J. Chao, S. J. Xiao, N. C. Seeman, *Nature* **2010**, *465*, 202 – 205.
[7] S. Pal, Z. T. Deng, B. Q. Ding, H. Yan, Y. Liu, *Angew. Chem.* **2010**, *122*, 2760 – 2764; *Angew. Chem. Int. Ed.* **2010**, *49*, 2700 – 2704.
[8] A. P. Alivisatos, K. P. Johnsson, X. Peng, T. E. Wilson, C. J. Loweth, M. P. Bruchez, Jr., P. G. Schultz, *Nature* **1996**, *382*, 609 – 611.
[9] M. M. Maye, M. T. Kumara, D. Nykypanchuk, W. B. Sherman, O. Gang, *Nat. Nanotechnol.* **2010**, *5*, 116 – 120.
[10] C. J. Loweth, W. B. Caldwell, X. G. Peng, A. P. Alivisatos, P. G. Schultz, *Angew. Chem.* **1999**, *111*, 1925 – 1929; *Angew. Chem. Int. Ed.* **1999**, *38*, 1808 – 1812.
[11] L. A. Stearns, R. Chhabra, J. Sharma, Y. Liu, W. T. Petuskey, H. Yan, J. C. Chaput, *Angew. Chem.* **2009**, *121*, 8646 – 8648; *Angew. Chem. Int. Ed.* **2009**, *48*, 8494 – 8496.
[12] A. J. Mastroianni, S. A. Claridge, A. P. Alivisatos, *J. Am. Chem. Soc.* **2009**, *131*, 8455 – 8459.
[13] J. Sharma, R. Chhabra, A. Cheng, J. Brownell, Y. Liu, H. Yan, *Science* **2009**, *323*, 112 – 116.
[14] M. Manchester, P. Singh, *Adv. Drug Delivery Rev.* **2006**, *58*, 1505 – 1522.
[15] M. Sara, U. B. Sleytr, *J. Bacteriol.* **2000**, *182*, 859 – 868.
[16] Y. Leng, H. P. Wei, Z. P. Zhang, Y. F. Zhou, J. Y. Deng, Z. Q. Cui, D. Men, X. Y. You, Z. N. Yu, M. Luo, X. E. Zhang, *Angew. Chem.* **2010**, *122*, 7401 – 7404; *Angew. Chem. Int. Ed.* **2010**, *49*, 7243 – 7246.
[17] A. Klug, *Angew. Chem.* **1983**, *95*, 579 – 596; *Angew. Chem. Int. Ed. Engl.* **1983**, *22*, 565 – 582.
[18] R. A. Miller, N. Stephanopoulos, J. M. McFarland, A. S. Rosko, P. L. Geissler, M. B. Francis, *J. Am. Chem. Soc.* **2010**, *132*, 6068 – 6074.
[19] J. Sun, C. DuFort, M. C. Daniel, A. Murali, C. Chen, K. Gopinath, B. Stein, M. De, V. M. Rotello, A. Holzenburg, C. C. Kao, B. Dragnea, *Proc. Natl. Acad. Sci. USA* **2007**, *104*, 1354 – 1359.
[20] T. Douglas, M. Young, *Nature* **1998**, *393*, 152 – 155.
[21] M. Comellas-Aragonès, H. Engelkamp, V. I. Claessen, N. A. Sommerdijk, A. E. Rowan, P. C. Christianen, J. C. Maan, B. J. Verduin, J. J. Cornelissen, R. J. Nolte, *Nat. Nanotechnol.* **2007**, *2*, 635 – 639.
[22] E. Dujardin, C. Peet, G. Stubbs, J. N. Culver, S. Mann, *Nano Lett.* **2003**, *3*, 413 – 417.
[23] Z. Y. Wu, A. Mueller, S. Degenhard, S. E. Ruff, F. Geiger, A. M. Bittner, C. Wege, C. E. Krill, *ACS Nano* **2010**, *4*, 4531 – 4538.
[24] R. Tsukamoto, M. Muraoka, M. Seki, H. Tabata, I. Yamashita, *Chem. Mater.* **2007**, *19*, 2389 – 2391.
[25] F. Li, Z. P. Zhang, J. Peng, Z. Q. Cui, D. W. Pang, K. Li, H. P. Wei, Y. F. Zhou, J. K. Wen, X. E. Zhang, *Small* **2009**, *5*, 718 – 726.
[26] D. L. Caspar, A. Klug, *Cold Spring Harbor Symp. Quant. Biol.* **1962**, *27*, 1 – 24.
[27] U. Neu, K. Woellner, G. Gauglitz, T. Stehle, *Proc. Natl. Acad. Sci. USA* **2008**, *105*, 5219 – 5224.
[28] S. K. Ghosh, T. Pal, *Chem. Rev.* **2007**, *107*, 4797 – 4862.
[29] S. Sheikholeslami, Y. W. Jun, P. K. Jain, A. P. Alivisatos, *Nano Lett.* **2010**, *10*, 2655 – 2660.
[30] K. H. Su, Q. H. Wei, X. Zhang, J. J. Mock, D. R. Smith, S. Schultz, *Nano Lett.* **2003**, *3*, 1087 – 1090.
[31] K. T. Shimizu, W. K. Woo, B. R. Fisher, H. J. Eisler, M. G. Bawendi, *Phys. Rev. Lett.* **2002**, *89*, 117401 – 117401.
[32] J. Lee, A. O. Govorov, J. Dulka, N. A. Kotov, *Nano Lett.* **2004**, *4*, 2323 – 2330.
[33] Q. B. Wang, H. N. Wang, C. X. Lin, J. Sharma, S. L. Zou, Y. Liu, *Chem. Commun.* **2010**, *46*, 240 – 242.
[34] J. Lee, T. Javed, T. Skeini, A. O. Govorov, G. W. Bryant, N. A. Kotov, *Angew. Chem.* **2006**, *118*, 4937 – 4941; *Angew. Chem. Int. Ed.* **2006**, *45*, 4819 – 4823.
[35] J. Lee, A. O. Govorov, N. A. Kotov, *Angew. Chem.* **2005**, *117*, 7605 – 7608; *Angew. Chem. Int. Ed.* **2005**, *44*, 7439 – 7442.
[36] T. Douglas, M. Young, *Science* **2006**, *312*, 873 – 875.
[37] S. E. Aniagyei, C. DuFort, C. C. Kao, B. Dragnea, *J. Mater. Chem.* **2008**, *18*, 3763 – 3774.
[38] F. Li, K. Li, Z. Q. Cui, Z. P. Zhang, H. P. Wei, D. Gao, J. Y. Deng, X. E. Zhang, *Small* **2010**, *6*, 2301 – 2308.

